Structural determinants of 5',6'-epoxyeicosatrienoic acid binding to and activation of TRPV4 channel

Alejandro Berna-Erro[a,1], Mercè Izquierdo-Serra[a,1], Romina V. Sepúlveda[b], Fanny Rubio-Moscardo[a], Pau Doñate-Macián[a], Selma A. Serra[a], Julia Carrillo-García[a], Alex Perálvarez-Marín[c], Fernando González-Nilo[b,d], José M. Fernández-Fernández [a,2] and Miguel A. Valverde[a,2]

[a]Laboratory of Molecular Physiology, Dept. of Experimental and Health Sciences, Universitat Pompeu Fabra, Barcelona, Spain.

[b]Universidad Andrés Bello, Center for Bioinformatics and Integrative Biology, Facultad de Ciencias Biológicas, Av. República 239, Santiago, Chile.

[c]Unitat de Biofísica, Centre d'Estudis en Biofísica, Departament de Bioquímica i de Biologia Molecular, Universitat Autònoma de Barcelona, 08193 Bellaterra, Spain

[d]Centro Interdisciplinario de Neurociencia de Valparaíso, Facultad de Ciencias, Universidad de Valparaíso, Valparaíso 2366103, Chile.

[1]Contributed equally to this work

[2]Corresponding authors: Prof. Miguel A. Valverde and Dr. José M. Fernandez-Fernández Laboratory of Molecular Physiology, Universitat Pompeu Fabra, C/ Dr. Aiguader 88, Barcelona 08003, Spain. Phone: 34 93 3160853, Fax: 34 93 3160901. Email: miguel.valverde@upf.edu ; jmanuel.fernandez@upf.edu

SUPPLEMENTARY INFORMATION

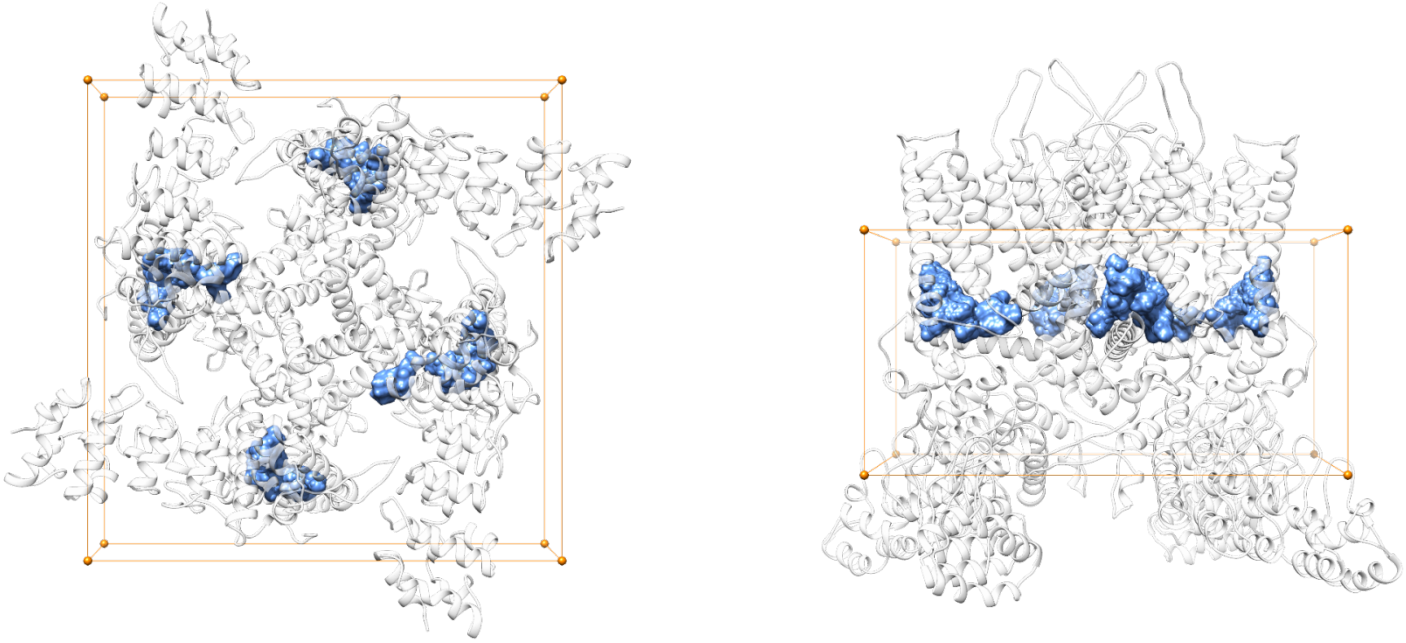

```
148 VFNRPILFDIVSRGSTADLDGLLPFLLTHKKRLTDEEFREPSTGKTCLPKALLNLSNGRN 207
208 DTIPVLLDIAERTGNMREFINSPFRDIYYRGQTALHIAIERRCKHYVELLVAQGADVHAQ 267
268 ARGRFFQPKDEGGYFYFGELPLSLAACTNQPHIVNYLTENPHKKADMRRQDSRGNTVLHA 327
328 LVAIADNTRENTKFVTKMYDLLLLKCARLFPDSNLEAVLNNDGLSPLMMAAKTGKIGIFQ 387
388 HIIRREVTDEDTRHLSRKFKDWAYGPVYSSLYDLSSLDTCGEEASVLEILVYNSKIENRH 447
448 EMLAVEPINELLRDKWRKFGAVSFYINVVSYLCAMVIFTLTAYYQPLEGTPPYPYRTTVD 507
508 YLRLAGEVITLFTGVLFFFTNIKDLFMKKCPGVNSLFIDGSFQLLYFIYSVLVIVSAALY 567
568 LAGIEAYLAVMVFALVLGWMNALYFTRGLKLTGTYSIMIQKILFKDLFRFLLVYLLFMIG 627
628 YASALVSLLNPCANMKVCNEDQTNCTVPTYPSCRDSETFSTFLLDLFKLTIGMGDLEMLS 687
688 STKYPVVFIILLVTYIILTFVLLLNMLIALMGETVGQVSKESKHIWKLQWATTILDIERS 747
748 FPVFLRKA 755
```

Figure supplement 1. 5',6'-EET blind docking. Top, TRPV4 bottom and side views (white ribbons) with 100 5',6'-EET docking poses (light blue surface) defining the putative binding site. The docking box of 100Å x 100 Å x 50 Å is indicated by the orange line box. **Bottom,** TRPV4 residues (green highlight) within a 5 Å distance of the 5,6-EET docking poses.

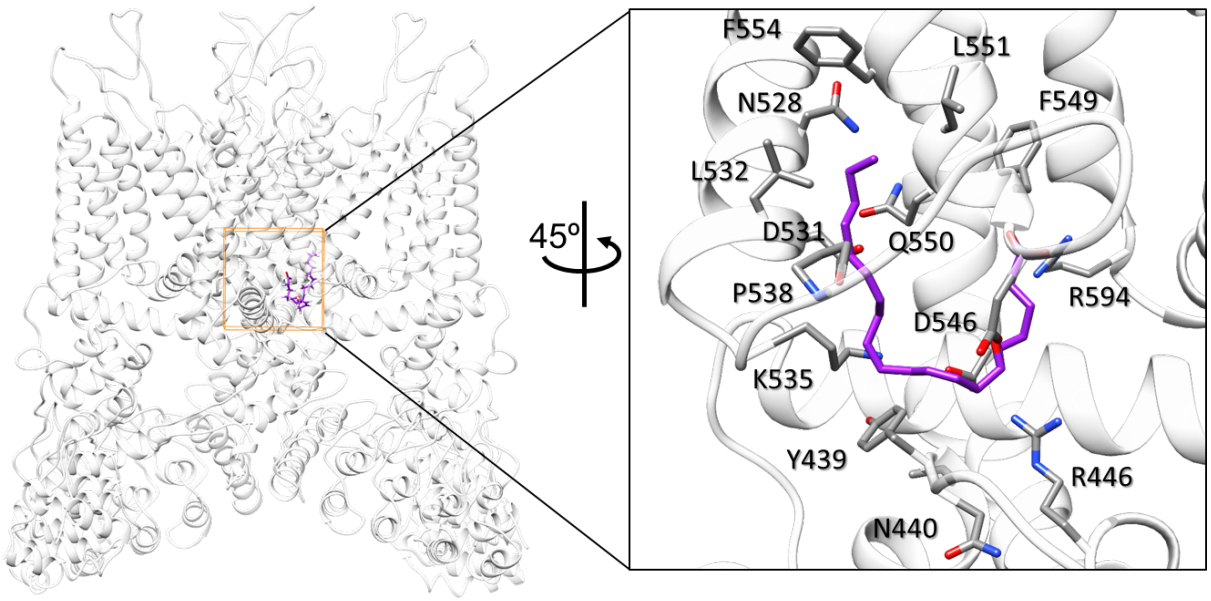

Figure supplement 2. 5',6'-EET refined docking. TRPV4 side view (white ribbons) with the 5',6'-EET highest energy docking solution (in purple) defining the putative binding site. The docking box of 20Å x 20 Å x 20 Å is indicated by the orange line box. The zoomed 5',6'-EET-binding site highlights the TRPV4 residues within a 3.5 Å distance of 5',6'-EET.

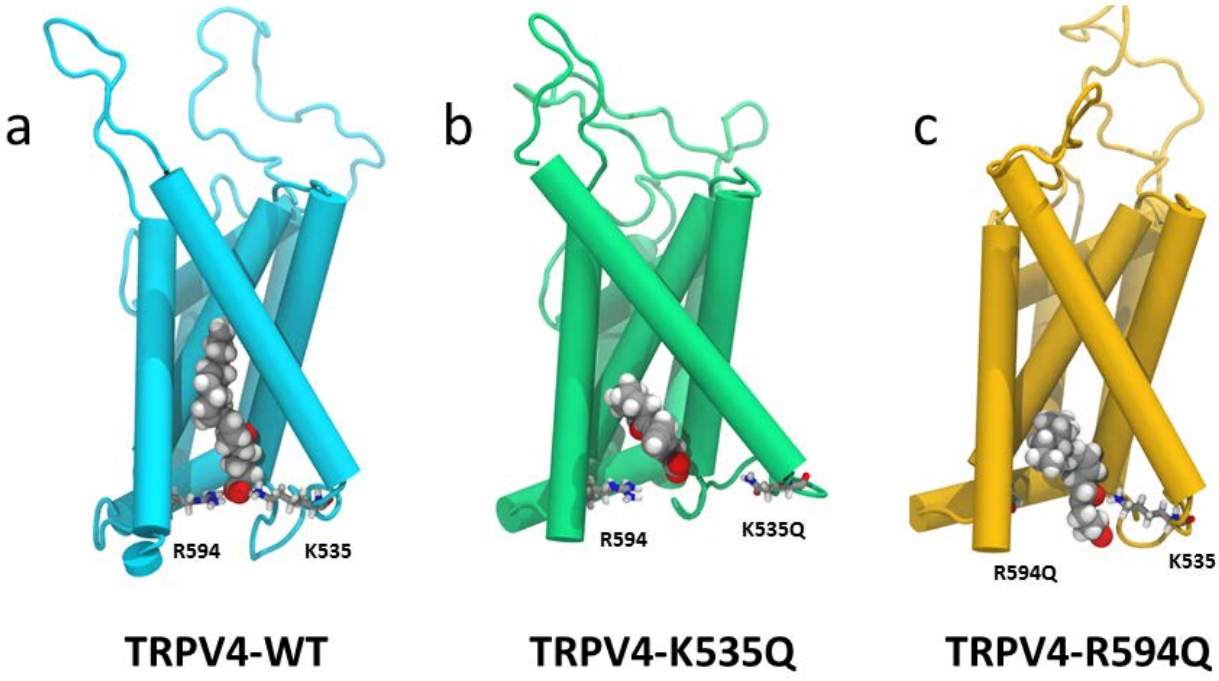

Figure supplement 3. Atomic-level interactions between 5',6'-EET and residues K535 and R594 of a single subunit in the TRPV4-WT (**a**), TRPV4-K535Q (**b**) and TRPV4-R594Q (**c**) systems. Note the increased distance between 5',6'-EET and the mutated residues K535Q and R594Q**.**

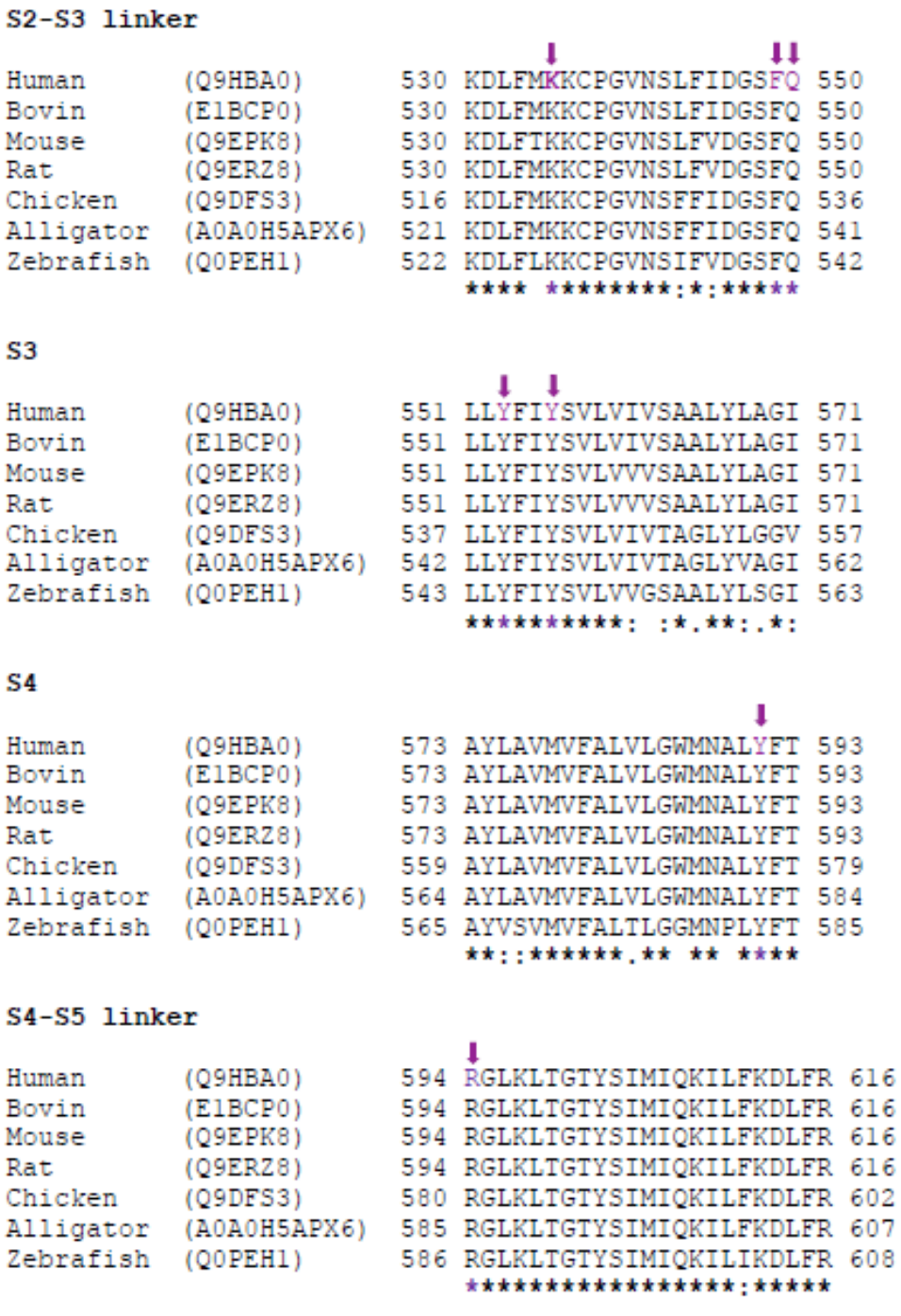

Figure supplement 4. Evolutionary conservation of TRPV4 regions relevant to EET binding. Sequence alignment of S2-S3 linker, S3, S4 and S4-S5 linker of TRPV4 from different species. Residues within a distance of 3.5 Å of EET (according to MD simulation) are shown in purple. Closed arrows indicate identical aa and open arrows conserved or semi-conserved aa. "*" identical residues; ":" conserved substitutions (same amino acid group); "." semi-conserved substitution (similar shapes).

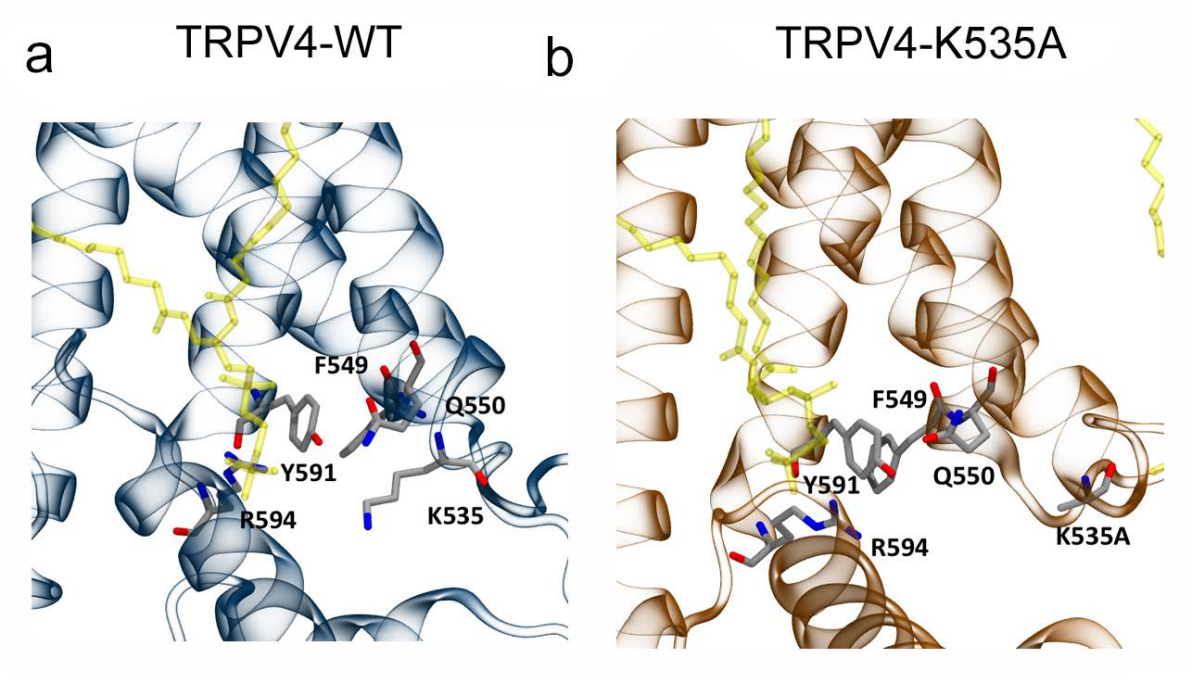

Supplementary Figure. 5. MD simulations in the absence of 5',6'-EET. Images of the predicted EET-binding site in TRPV4-WT (a) and TRPV4 K535A (b) in the absence of 5',6'-EET. In yellow are the membrane lipids (POPC) present in the simulation. Note that the predicted EET binding site is empty in both systems.

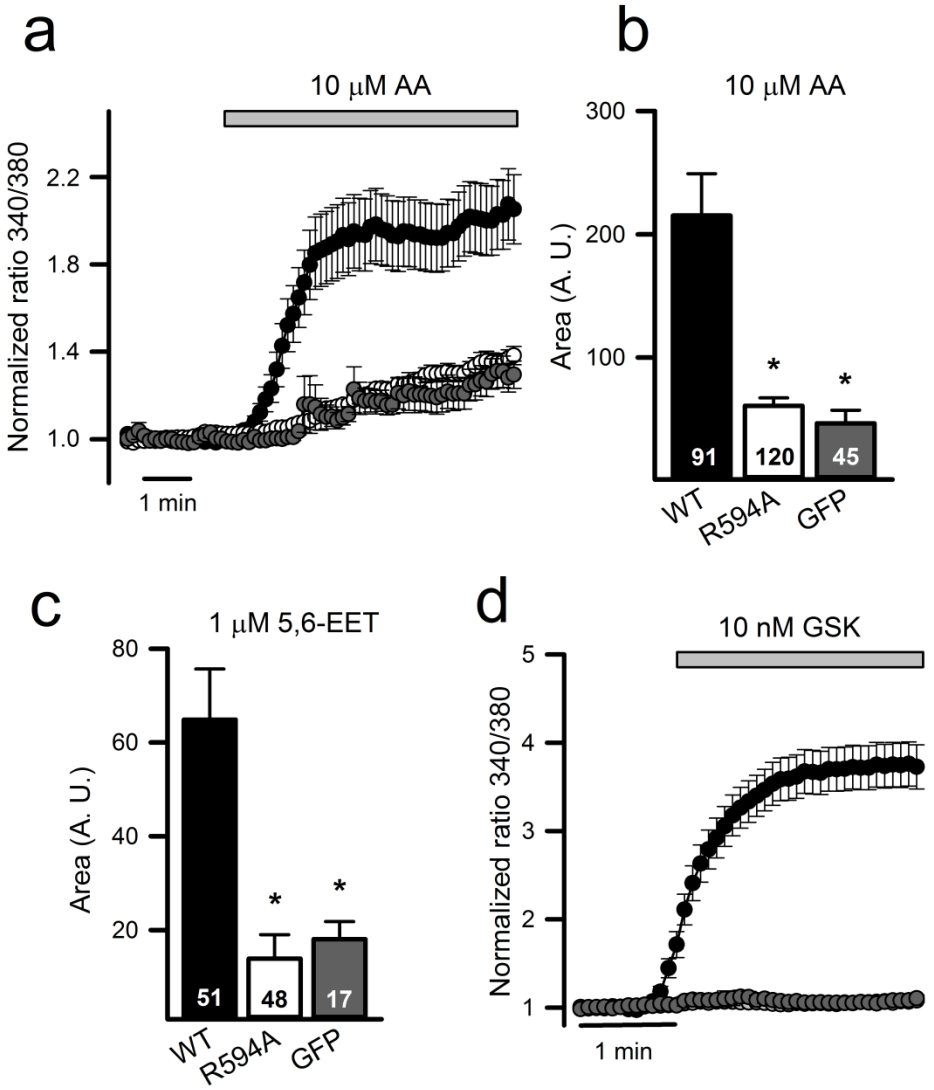

Figure supplement 6. TRPV4-R594A lacks activation by 5',6'-EET, AA and GSK1016790A. Changes in intracellular [Ca^{2+}] (indicated by normalized fura-2 ratios and areas under the curves) in HeLa cells transfected with GFP, TRPV4-WT or TRPV4-R594A cDNAs, after perfusion with 10 μM AA (**a,b**), 1 μM 5,6-EET (**c**) and 10 nM GSK1016790A (**d**). Numbers inside the bars indicate the number of cells analyzed. Means ± S.E.M. *P<0.05 when compared with cells expressing TRPV4-WT channels (Kruskal-Wallis One Way Analysis of Variance **f**ollowed by Dunn's method of multiple comparisons).

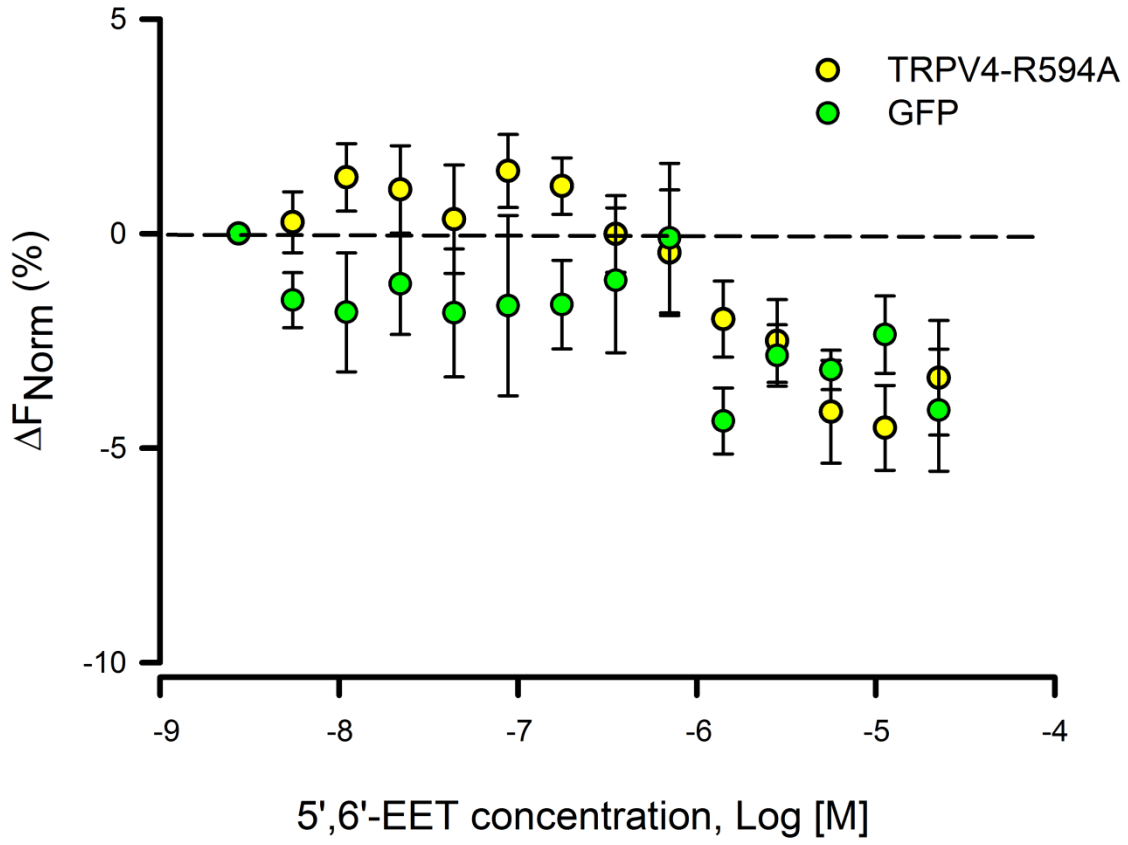

Figure Supplement 7. Thermophoretic analysis of the TRPV4-EET interaction.
Average changes in normalized fluorescence obtained for GFP-labeled TRPV4-R594A (n=5) or GFP (n=5) plotted against 5',6'-EET concentration.

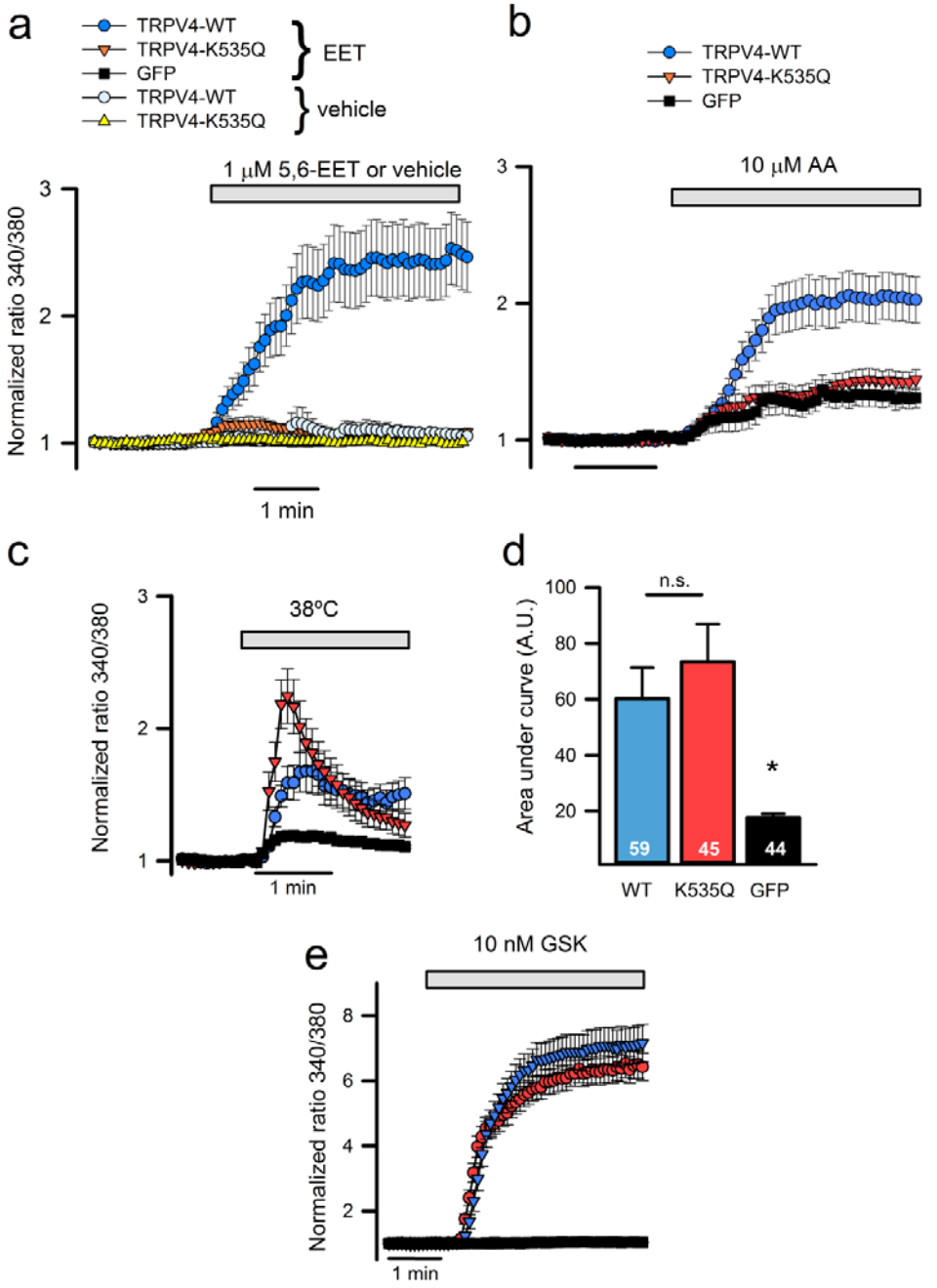

Figure supplement 8. K535Q substitution abolishes TRPV4 activation by 5',6'-EET and AA, but not by heat or GSK1016790A agonist. Intracellular Ca^{2+} changes (indicated by fura-2 ratios) in HeLa cells transfected with GFP (n=50), TRPV4-WT (n=77) or TRPV4-K535Q (n=74) cDNAs, after perfusion with 1 μM 5,6-EET or vehicle (WT, n=51; K535Q, n=20) **(a)**, 10 μM AA (GFP (n=66), TRPV4-WT (n=90) or TRPV4-K535Q (n=90)) (**b**), warm solution (38 ºC) **(c-d)** and 10 nM GSK1016790A (n= 44-59) **(e)**. Means ± S.E.M. *P<0.05 or not significant (n.s.) when compared with cells expressing TRPV4 WT channels (Kruskal-Wallis One Way Analysis of Variance **f**ollowed by Dunn's method of multiple comparisons).

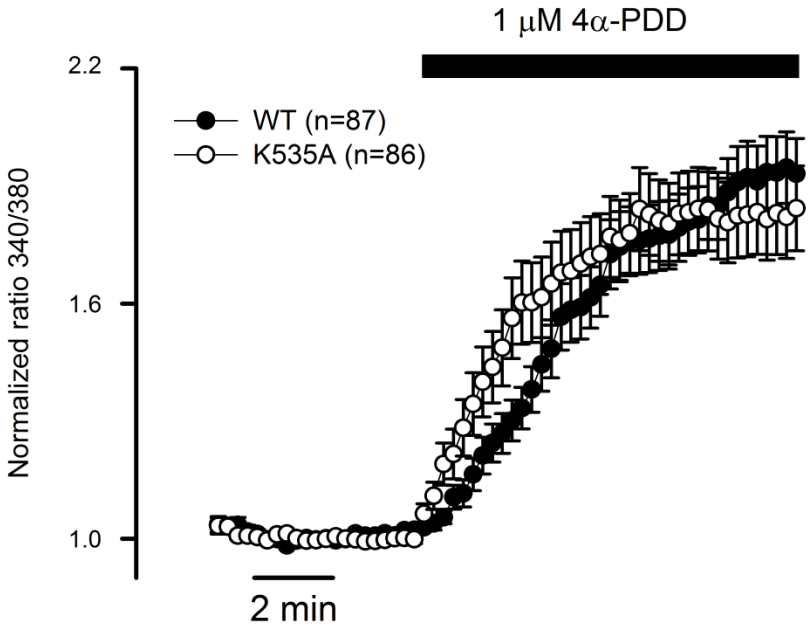

Figure supplement 9. K535A substitution does not abolish TRPV4 activation by 4α-PDD. (A), Fura-2 ratios obtained in HeLa cells transfected with TRPV4-WT (n=87) or TRPV4-K535A (n=86) cDNAs, after perfusion with 10 μM 4α-PDD. Traces showing means ± SEM..

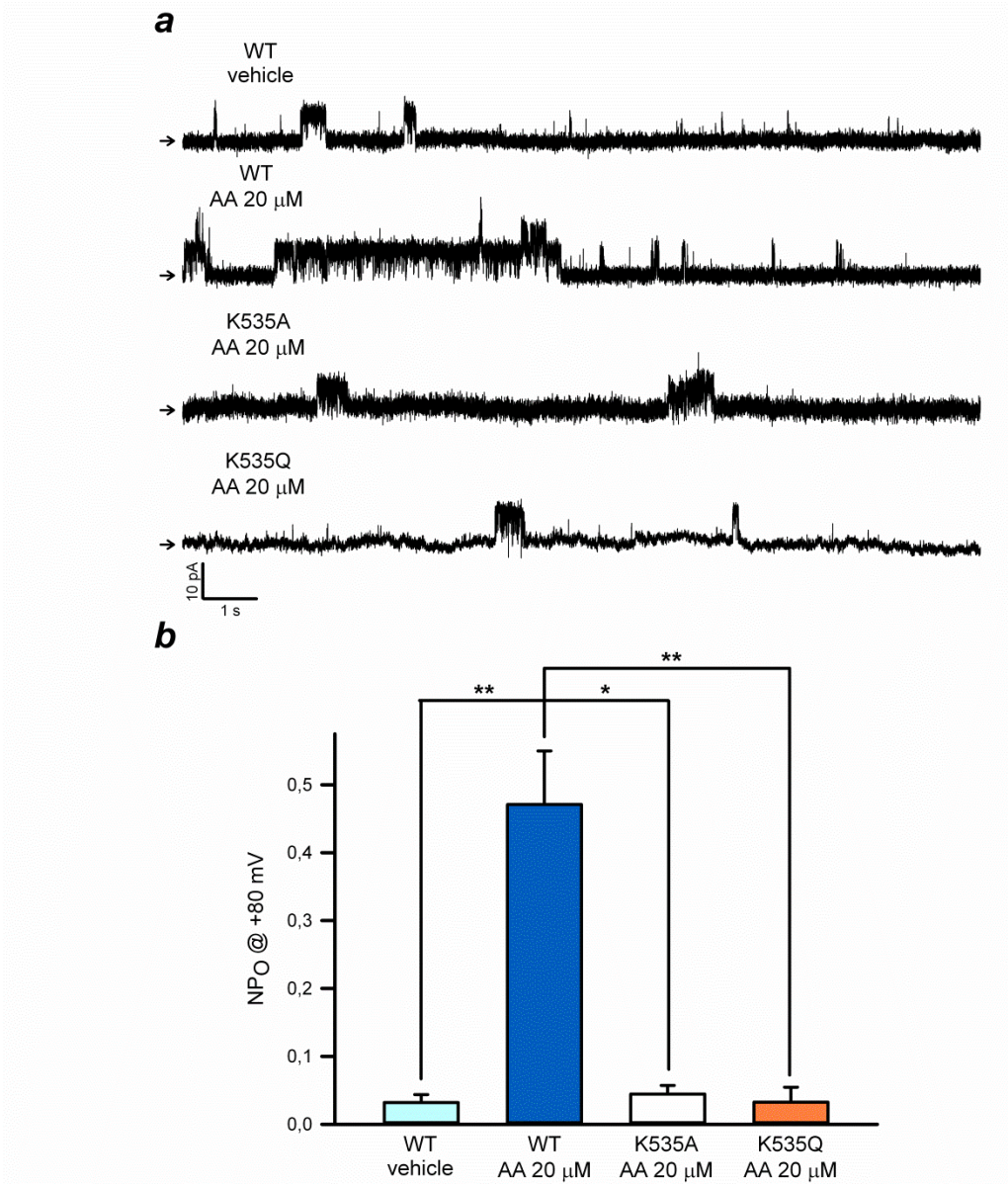

Figure supplement 10. AA increases open probability of WT but not K535 mutant TRPV4 channels. (a) Representative 15 s recordings obtained from cell-attached patches clamped at +80mV in HEK293 cells expressing WT, K535A or K535Q TRPV4 mutant channels in the presence of extracellular vehicle (DMSO 1:500) or Arachidonic Acid (AA 20 μM), as stated. Arrows indicates the closed state level. **(b)** Average open probability (NP_O) (expressed as the mean ± SEM) of WT and K535 mutant TRPV4 channels at the experimental conditions indicated above (vehicle, n=6; WT, n=11; K535A, n=7; K535Q, n=6). **P<0.01, *P<0.05 (Kruskal-Wallis followed by Dunn *post hoc* test).

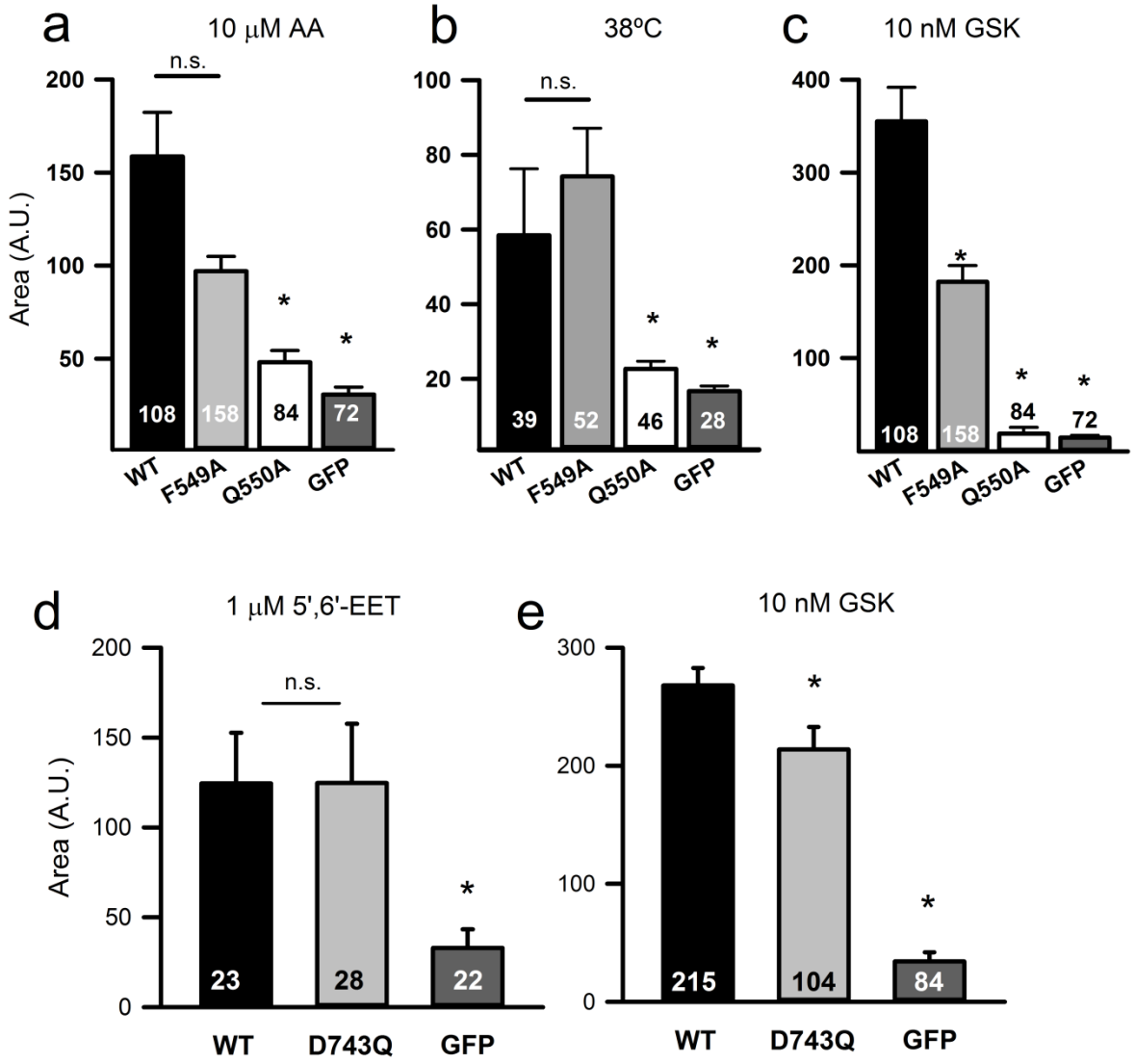

Figure supplement 11. Average $[Ca^{2+}]_i$ increases (area under the curve) obtained from cells expressing TRPV4-WT, TRPV4-F549A, TRPV4-Q550A, TRPV4-D743Q or GFP and exposed to 10 μM AA (**a**), 38ºC (**b**), 10 nM GSK1016790A (**c,e**) and 1 μM 5',6'-EET (**d**). Numbers inside the bars indicate the number of cells analyzed. *P < 0.05 or not significant (n.s.) when compared with cells expressing TRPV4 WT channels (one way ANOVA followed by Bonferroni *post hoc* test).

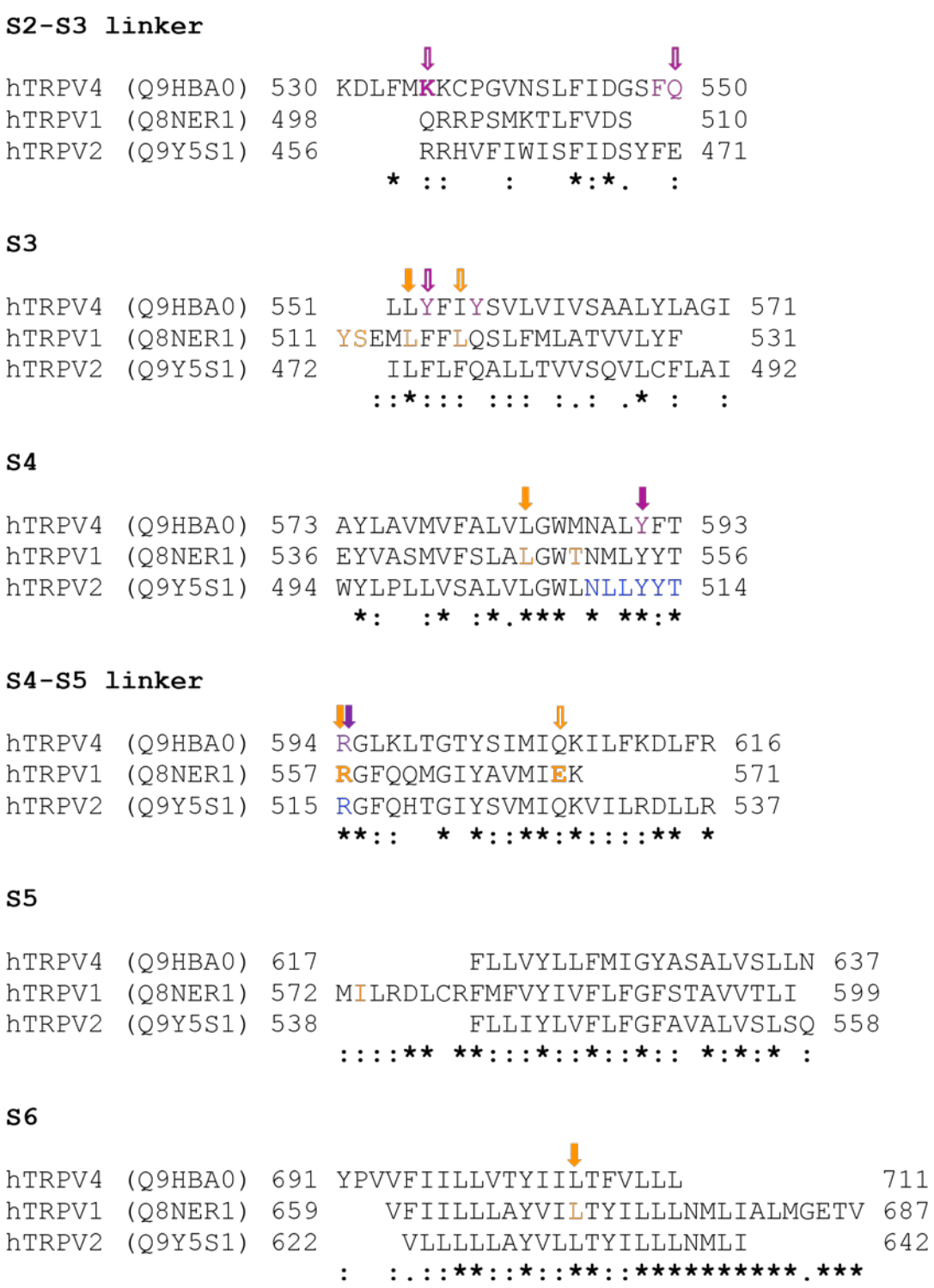

Figure supplement 12. Comparison of human TRPV4, TRPV1 and TRPV2 sequences involved in binding of EET, capsaicin and lipids, respectively. Sequence alignment of S2-S3 linker, S3, S4, S4-S5 linker and S6 of human TRPV4, TRPV1 and TRPV2 channels. TRPV4 residues predicted to be within a distance of 3.5 Å of EET are shown in purple. TRPV1 residues involved in the binding of capsaicin are displayed in orange [59]. TRPV2

amino acids around the C-terminal region of S4 involved in lipid binding [58] (with some overlap with the binding-pocket for vanilloids at TRPV1) are depicted in blue. Closed arrows indicating those amino acids that are identical and open arrows pointing the conserved or semiconserved residues. “*” identical residues; “:” conserved substitutions (same amino acid group); “.” semi-conserved substitution (similar shapes).